

Compressibility of synthetic potassium-rich clinopyroxene: In-situ high-pressure single-crystal X-ray study

LUCA BINDI,^{1,*} ROBERT T. DOWNS,² GEORGE E. HARLOW,³ OLEG G. SAFONOV,⁴ YURIY A. LITVIN,⁴ LEONID L. PERCHUK,⁵ HINAKO UCHIDA,² AND SILVIO MENCHETTI¹

¹Dipartimento di Scienze della Terra, Università di Firenze, Via La Pira 4, I-50121, Firenze, Italy

²Department of Geosciences, University of Arizona, Tucson, Arizona 85721-0077, U.S.A.

³Department of Earth and Planetary Sciences, American Museum of Natural History, New York, New York 10024-5192, U.S.A.

⁴Institute of Experimental Mineralogy, Moscow district, 142432, Chernogolovka, Russia

⁵Department of Geology, Moscow State University, Vorobievsky Gory, 119899, Moscow, Russia

ABSTRACT

The crystal structure of a synthetic potassium-rich clinopyroxene, $(\text{Ca}_{0.88}\text{K}_{0.12})(\text{Mg}_{0.83}\text{Al}_{0.17})(\text{Si}_{1.98}\text{Al}_{0.02})\text{O}_6$, was studied using high-pressure single-crystal X-ray diffraction methods. A four-pin diamond anvil cell with 4:1 methanol:ethanol pressure medium was used to achieve pressures to 9.72 GPa. Unit-cell data were measured at 17 pressures, and intensity data were collected at 6 pressures. Fitting the P - V data to the third-order Birch-Murnaghan equation of state yields $V_0 = 435.49(3) \text{ \AA}^3$, $K_0 = 129(1) \text{ GPa}$, $K' = 2.7(3)$. Anisotropic compression was observed with unit strain axial ratios of 1:1.94:1.90. Unit-cell parameters decrease gradually as a function of pressure with axial compressibilities $\beta_b > \beta_c \sim \beta_a$. They match those found for kosmochlor but are stiffer than those observed for synthetic diopside and hedenbergite. Compressibilities of the bond distances within the M2, M1, and T polyhedra show significant anisotropy. The incorporation of K into the clinopyroxene structure has little effect on its compressibility, although the concomitant substitution of Al in M1 from the K-Jd component reduces its compressibility. The K atom is softer than the M2 polyhedron and thus shrinks enough at high pressure to fit into the pyroxene structure.

Keywords: High-pressure studies, clinopyroxene, crystal structure, XRD data, chemical mineral analysis

INTRODUCTION

Potassium-rich clinopyroxenes (KCpx) occur as inclusions in diamonds, in eclogitic and peridotitic xenoliths from kimberlites and lamproites (Bishop et al. 1978; Harlow and Veblen 1991; Reid et al. 1976; Jaques et al. 1990), as rare megacrysts in some K-rich volcanics (Ghorbani and Middlemost 2000), and as inclusions in garnets of garnet-clinopyroxene rocks from the Kokchetav Ultra High Pressure (UHP) Complex, Northern Kazakhstan (e.g., Sobolev and Shatsky 1990). The concentration of K_2O in natural clinopyroxenes (for example, inclusions in diamonds) does not usually exceed 1.7 wt% (Harlow and Veblen 1991). Nevertheless, Bindi et al. (2003) recently reported a concentration of K_2O , 3.61 wt%, for a clinopyroxene crystal included in garnet from a garnet-clinopyroxene rock of the Kumdy-Kol microdiamond mine, Kokchetav UHP Complex. Experiments in model and natural systems at $P > 5 \text{ GPa}$ (see review in Perchuk et al. 2002) indicate that 3.61 wt% is not a limit for the K_2O content in clinopyroxene. Chudinovskikh et al. (2001), Safonov et al. (2002, 2003), and Bindi et al. (2002), reported 5.50–5.75 wt% of K_2O in clinopyroxene in the run products in both carbonate-silicate and alumino-silicate systems at 7 GPa. All the above data demonstrate that clinopyroxene is a leading host for potassium at UHP and mantle conditions. Therefore, how clinopyroxene

can incorporate potassium at high-pressures is important to the understanding of the behavior of K in the deep Earth.

Modifications due to high-potassium content in $C2/c$ clinopyroxene structure at ambient pressure were studied in detail on synthetic (Bindi et al. 2002) and natural crystals (Harlow 1996; Bindi et al. 2003). These authors point out that the substitution of K for Ca is accompanied by significant, but expected, modifications to the average structure, mainly a lengthening of the M2-O3C1 bond distance and a shortening of the T-O3A1 bond distance. Bindi et al. (2002, 2003) did not find evidence for a small cation, such as Mg, coexisting with Ca in the M2 site that might act as a structural stabilizer for the accommodation of K in the clinopyroxene structure. Harlow (1996) has proposed that the average size of a small cation plus the large K atom would approximate the size of Ca and thus reduce lattice strain.

Harlow (1997) suggested that the polyhedral compressibility of K^+ is significant and at pressures above 5 GPa the potassium ion might easily substitute for Ca^{2+} . To preserve charge balance in the structure, introduction of K^+ into the M2 site should be accompanied by the simultaneous replacement of $(\text{Mg}, \text{Fe})^{2+}$ in the M1 site by a trivalent cation (e.g., Al, Cr) according to the scheme $\text{Ca}_{\text{M2}}(\text{Mg}, \text{Fe})_{\text{M1}} \leftrightarrow \text{K}_{\text{M2}}(\text{Al}, \text{Cr})_{\text{M1}}$. This scheme, which is supported by a direct correlation of K content with trivalent cations in both natural and synthetic clinopyroxenes (e.g., Edgar and Vukadinovic 1993; Perchuk et al. 1996; Safonov et al. 2002, 2003, 2005), reflects the presence of the fictive K-jadeite

* E-mail: lbindi@geo.unifi.it

(KAlSi₂O₆) and K-kosmochlor (KCrSi₂O₆) end-members in the clinopyroxene solid solution.

The purpose of the present study is to investigate the influence of potassium on the M1 and M2 sites in the clinopyroxene structure at high pressure by means of a single-crystal high-pressure X-ray study on a synthetic crystal with chemical composition (Ca_{0.88}K_{0.12})(Mg_{0.83}Al_{0.17})(Si_{1.98}Al_{0.02})O₆. Compressibility data for all of the end-member Cpx minerals do not yet exist and predictions for structures as complex as natural Cpx are, indeed, extrapolations.

SYNTHESIS

The potassium-rich clinopyroxene studied here was synthesized during run 939 at *P* = 7 GPa, *T* = 1480 °C and 510 min duration from a mixture of stoichiometric gels of CaMgSi₂O₆ and KAlSi₂O₆ compositions prepared using the nitrate method (Hamilton and Henderson 1968). About 20 mg was placed into a Pt capsule and subsequently dried for several hours at 110 °C. The run was performed at the Institute of Experimental Mineralogy of the Russian Academy of Sciences with the high-pressure “anvil-with-hole” apparatus (Litvin 1990) using a high-pressure cell made of marble and equipped with a graphite heater of dimension 7.2 mm in length, 7.5 mm in diameter, and 0.75 mm wall thickness. Details of the experimental technique and cell calibration are described in Safonov et al. (2003, 2005). After the run, a sample was embedded in epoxy and polished for a study of texture and composition using a microprobe. Crystals of potassium-bearing clinopyroxene of approximately 400 μm in size were observed among smaller elongated clinopyroxene and euhedral pyrope-grossular garnet crystals (Fig. 1). The phase assemblage is in good agreement with the phase diagram for the join CaMgSi₂O₆-KAlSi₂O₆ at 7 GPa (Safonov et al. 2003), implying that the potassium-bearing clinopyroxenes of run 939 are equilibrium products of the experiment.



FIGURE 1. BSE image of euhedral clinopyroxene crystals, coexisting with garnet (small euhedral grains in the matrix), produced in the run 939 (*T* = 1480 °C, *P* = 7 GPa). CamScan electronic microscope.

EXPERIMENTAL METHODS

A sample of KCpx (labeled 939-1), originally 130 × 160 × 420 μm in size, was broken into smaller fragments, suitable for diamond anvil study. The crystals were untwinned and exhibited ideal scan profiles with narrow Gaussian full-widths of 0.08° in ω. The crystal was mounted on a Picker diffractometer with unfiltered Mo radiation, automated with a Windows-based Visual-Fortran code extensively modified after the SINGLE software (Angel et al. 2000).

The peak positions of 22 strong reflections with 13 < 2θ < 30° were determined by the 8-reflection centering technique of King and Finger (1979) with the modification of fitting to the sum of 2 Gaussian profiles that represent Kα1 and Kα2 scattering constrained by separation and relative intensity. Refined cell parameters are listed in Table 1. Half a sphere of intensity data were collected to 2θ ≤ 60°, using ω scans of 1° width, step size of 0.025° and 3 s per step counting times. The structure was refined on *F* with anisotropic displacement factors using a modification of RFINE (Finger and Prince 1975) to an *R*_w = 0.016. In addition, for consistency with the high-pressure data, the structure was refined with isotropic displacement factors to an *R*_w = 0.054. Structure factors were weighted by *w* = [σ_F² + (*pF*)²]⁻¹, where σ_F was obtained from counting statistics and *p* chosen to ensure normally distributed errors (Ibers and Hamilton 1974). An isotropic extinction correction was also applied. Structural data at room conditions are summarized in Table 2.

The crystal was loaded into a four-pin Merrill Basset type diamond anvil cell with the normal to the cleavage plane (110) parallel to the cell axis. The diamond anvil culet was 600 μm in diameter. A stainless steel gasket, 250 μm thick, pre-indentated to 100 μm, with a hole of 300 μm diameter was used. A mixture of 4:1 methanol:ethanol was used as a pressure medium. To determine pressure, a small ruby fragment was loaded in the cell, and the positions of its R1 and R2 peaks were determined by fitting Lorentzian functions to the fluorescence spectra. The pressure was determined by the equation of Mao et al. (1978) with an estimated error of 0.05 GPa.

Unit-cell parameters and volume were determined by 8-position centering of 36 accessible reflections in the interval 12° < 2θ < 45° at 16 different pressures to 9.72 GPa (Table 1). Every accessible reflection allowed by *C2/c* symmetry was collected to 2θ ≤ 60° at 6 different pressures to 9.72 GPa, with ω scans of 1° width, in steps of 0.025°, and counting times of 10 s per step using the fixed φ-mode for data collection (Angel et al. 2000). These data reduced to ~330 symmetry equivalent reflections. Absorption corrections for the Be seats and diamond anvils were made from a transmission profile of the diamond cell before loading. Intensity data were processed as noted above at room conditions. The crystal structure refinement data are summarized in Table 3. For each refinement, a distinct value of *p* was obtained to adjust the weighting scheme, as mentioned above, to produce a normalized error distribution. This procedure usually produces a larger value of *R*_w than would have resulted with *p* = 0, but the refined structure parameters vary more smoothly over the pressure range of the experiment (Angel et al. 2000). Bond lengths and angles reported in Table 4 were calculated using BOND91 software, modified after Finger and Prince (1975). Polyhedral volumes were obtained with XTALDRAW (Downs and Hall-Wallace 2003).

TABLE 1. Unit-cell parameters as a function of pressure for the KCpx crystal

Run	<i>P</i> (GPa)	<i>a</i>	<i>b</i>	<i>c</i>	β	<i>V</i> (Å ³)
P0-air*	0.0001	9.6912(3)	8.8986(3)	5.2531(3)	105.990(3)	435.49(3)
P1*	0.46	9.6828(4)	8.8880(4)	5.2482(3)	105.951(4)	434.27(4)
P2	1.00	9.6660(5)	8.8699(4)	5.2399(4)	105.883(4)	432.09(4)
P3	1.78	9.6459(4)	8.8487(4)	5.2294(3)	105.802(4)	429.49(3)
P4*	2.45	9.6313(5)	8.8327(4)	5.2212(3)	105.746(5)	427.50(4)
P5	3.06	9.6165(5)	8.8154(3)	5.2132(2)	105.689(4)	425.48(3)
P6	3.86	9.5982(4)	8.7961(2)	5.2038(2)	105.628(4)	423.09(2)
P7	4.62	9.5828(5)	8.7776(2)	5.1949(2)	105.571(4)	420.93(3)
P8*	5.36	9.5674(5)	8.7596(3)	5.1863(2)	105.520(5)	418.79(3)
P9	5.81	9.5566(6)	8.7472(3)	5.1801(2)	105.484(5)	417.30(3)
P10	6.61	9.5384(4)	8.7271(2)	5.1704(1)	105.434(4)	414.87(2)
P11	7.41	9.5217(5)	8.7080(2)	5.1612(2)	105.381(4)	412.61(3)
P12*	8.11	9.5089(6)	8.6937(3)	5.1545(2)	105.344(6)	410.91(3)
P13	8.79	9.4971(7)	8.6799(3)	5.1474(2)	105.317(6)	409.25(4)
P14	9.16	9.4909(8)	8.6686(4)	5.1427(3)	105.292(7)	408.12(4)
P15	9.48	9.4821(7)	8.6601(3)	5.1387(2)	105.273(6)	407.07(4)
P16*	9.72	9.4762(4)	8.6541(2)	5.1356(2)	105.269(4)	406.29(2)

Notes: *V*₀ = 435.49(3) Å³, *K*₀ = 129(1), *K*' = 2.7(3). *V*₀ = 435.52(3) Å³, *K*₀ = 123.7(3), *K*' = 4.

* Intensity data collected at this pressure.

TABLE 2. Structural parameters for the KCpx in air at room conditions

Atom	x	y	z	$B_{eq}(\text{\AA}^2)$	β_{11}	β_{22}	β_{33}	β_{12}	β_{13}	β_{23}
M2	0	0.30245(4)	¼	0.896(9)	0.00315(4)	0.00222(4)	0.00716(14)	0	-0.00010(6)	0
M1	0	0.90703(7)	¼	0.51(1)	0.00143(6)	0.00169(7)	0.00454(20)	0	0.00042(9)	0
T	0.28620(4)	0.09297(4)	0.22578(6)	0.427(8)	0.00115(4)	0.00151(4)	0.00400(12)	0.00002(3)	0.00061(5)	-0.00017(5)
O1	0.11410(9)	0.08445(11)	0.13811(18)	0.83(2)	0.00128(9)	0.00394(12)	0.00797(33)	0.00025(8)	0.00105(14)	-0.00028(16)
O2	0.35996(11)	0.25132(11)	0.31167(20)	0.94(2)	0.00364(11)	0.00202(10)	0.00935(34)	-0.00071(8)	0.00189(15)	-0.00077(15)
O3	0.35013(9)	0.01660(10)	0.99295(17)	0.69(1)	0.00166(9)	0.00281(11)	0.00628(31)	-0.00006(8)	0.00109(14)	-0.00104(15)

Notes: $R_w = 1.6\%$.**TABLE 3.** Structural parameters for KCpx as a function of pressure

P(GPa)	P0 = 0.0001	P1 = 0.46	P4 = 2.45	P8 = 5.36	P12 = 8.11	P16 = 9.72
R_{int}	0.012	0.027	0.031	0.036	0.033	0.031
R_w	0.054	0.057	0.052	0.052	0.052	0.052
M2 y	0.30244(8)	0.3025(2)	0.3036(2)	0.3044(2)	0.3053(2)	0.3058(1)
B(iso)	0.87(2)	1.05(4)	1.00(3)	1.29(4)	0.85(4)	0.79(3)
M1 y	0.9070(1)	0.9070(3)	0.9077(2)	0.9087(2)	0.9091(2)	0.9098(2)
B(iso)	0.52(3)	0.66(5)	0.62(4)	0.98(5)	0.63(5)	0.55(4)
Si x	0.28611(7)	0.2861(2)	0.2858(2)	0.2860(3)	0.2863(3)	0.2862(3)
y	0.09289(7)	0.0931(2)	0.0935(1)	0.0941(1)	0.0947(1)	0.0948(1)
z	0.2257(1)	0.2254(2)	0.2248(2)	0.2249(3)	0.2247(3)	0.2247(2)
B(iso)	0.43(2)	0.60(3)	0.59(3)	0.96(4)	0.54(4)	0.53(3)
O1 x	0.1140(2)	0.1146(5)	0.1142(5)	0.1119(8)	0.1136(8)	0.1124(7)
y	0.0844(2)	0.0845(4)	0.0849(4)	0.0846(4)	0.0853(4)	0.0852(3)
z	0.1382(4)	0.1375(7)	0.1386(7)	0.1370(8)	0.1385(8)	0.1385(7)
B(iso)	0.91(3)	1.02(7)	1.03(7)	1.40(7)	0.95(7)	0.86(6)
O2 x	0.3596(2)	0.3607(6)	0.3599(5)	0.3582(7)	0.3594(7)	0.3588(6)
y	0.2514(2)	0.2523(5)	0.2533(4)	0.2549(4)	0.2566(4)	0.2577(4)
z	0.3113(4)	0.3124(8)	0.3131(7)	0.3144(9)	0.3155(8)	0.3170(6)
B(iso)	0.94(3)	1.08(7)	1.05(7)	1.36(7)	0.98(7)	0.93(6)
O3 x	0.3501(2)	0.3500(5)	0.3509(5)	0.3520(7)	0.3529(8)	0.3541(6)
y	0.0165(2)	0.0167(4)	0.0178(4)	0.0190(4)	0.0207(4)	0.0211(3)
z	0.9926(3)	0.9932(7)	0.9910(7)	0.9880(8)	0.9873(8)	0.9872(7)
B(iso)	0.67(3)	0.91(7)	0.83(6)	1.12(7)	0.81(7)	0.72(6)

Notes: $x_{M1} = x_{M2} = 0$; $z_{M1} = z_{M2} = ¼$. M2 = $Ca_{0.88}K_{0.12}$; M1 = $Mg_{0.83}Al_{0.17}$; T = $Si_{0.99}Al_{0.01}$.**TABLE 4.** Selected bond lengths (angstroms), volume (\AA^3), and angles ($^\circ$) from structure refinements

P(GPa)	P0 = 0.0001 ^δ	P0 = 0.0001*	P1 = 0.46	P4 = 2.45	P8 = 5.36	P12 = 8.11	P16 = 9.72
R(SiO1)	1.6051(9)	1.605(2)	1.598(5)	1.592(5)	1.607(7)	1.586(7)	1.591(6)
R(SiO2)	1.588(1)	1.588(2)	1.597(5)	1.592(4)	1.583(5)	1.585(5)	1.585(4)
R(SiO3a)	1.6611(9)	1.663(2)	1.657(4)	1.657(4)	1.660(4)	1.650(4)	1.650(4)
R(SiO3b)	1.6808(9)	1.679(2)	1.683(4)	1.678(4)	1.668(5)	1.669(4)	1.667(4)
<R(SiO)>	1.6274	1.6338	1.6338	1.6302	1.6294	1.6224	1.6234
V(SiO ₄)	2.2013	2.220	2.219	2.204	2.201	2.173	2.176
R(M2O1)	2.385(1)	2.345(2)	2.386(4)	2.372(4)	2.352(5)	2.343(5)	2.329(4)
R(M2O2)	2.377(1)	2.380(2)	2.372(4)	2.368(4)	2.361(5)	2.347(5)	2.339(4)
R(M2O3c)	2.5463(9)	2.547(2)	2.544(4)	2.533(4)	2.521(5)	2.509(5)	2.495(4)
R(M2O3d)	2.7115(9)	2.711(2)	2.709(4)	2.668(4)	2.619(5)	2.578(5)	2.555(4)
Δ	0.1652	0.164	0.165	0.135	0.098	0.069	0.060
<R(M2O)>	2.5050	2.5056	2.5031	2.4851	2.4631	2.4439	2.4294
R(M1O1a)	2.102(1)	2.101(2)	2.105(4)	2.085(4)	2.049(5)	2.042(5)	2.022(4)
R(M1O1b)	2.0355(9)	2.036(2)	2.033(4)	2.030(4)	2.007(5)	2.009(5)	1.999(4)
R(M1O2)	2.027(1)	2.028(2)	2.015(5)	2.008(4)	2.003(5)	1.974(5)	1.971(5)
<R(M1O)>	2.0549	2.0550	2.0508	2.0406	2.0196	2.0085	1.9973
V(M1O ₆)	11.455	11.456	11.390	11.223	10.865	10.703	10.520
Si-O3-Si	136.53(6)	136.46(13)	136.56(32)	135.7(3)	134.8(5)	134.3(5)	133.5(4)
O3-O3-O3	167.17(8)	167.21(16)	167.09(33)	166.3(3)	165.4(3)	164.1(3)	163.8(2)

Notes: δ Structure at 0.0001 GPa, refined with anisotropic temperature factors.* Structure at 0.0001 GPa, refined with isotropic temperature factors. $\Delta = [R(M2O3d) - R(M2O3c)]$. The O3a in SiO₃ a is at [0.352,0.008,0.012]. The O3c in M2O3c is at [0.148,0.508,0.488]. The O1a in M1O1a is at [0.114,1.079,0.138].

CHEMICAL COMPOSITION

The same crystal used for the high-pressure study was analyzed by means of a JEOL JXA-8600 electron microprobe. Major and minor elements were determined at 15 kV accelerating voltage and 10 nA beam current, with 40 s counting times.

The matrix correction was performed with the Bence and Albee (1968) program as modified by Albee and Ray (1970). Replicate analyses of augite USNM 122142 were used to check accuracy and precision. The estimated analytical precision is: ± 0.02 for CaO and MgO; ± 0.03 for SiO₂; ± 0.06 for K₂O; ± 0.1 for Al₂O₃.

The standards employed were: olivine (Mg), diopside (Ca), albite (Al, Si), and sanidine (K). The crystal was found to be homogeneous within the analytical uncertainty. The average chemical composition (ten analyses on different spots) is reported in Table 5. On the basis of 6 O atoms, the formula is $(\text{Ca}_{0.88}\text{K}_{0.12})(\text{Mg}_{0.83}\text{Al}_{0.17})(\text{Si}_{1.98}\text{Al}_{0.02})\text{O}_6$.

RESULTS AND DISCUSSION

A pressure-volume equation of state was obtained by a non-linear fit of the weighted data from Table 1 to a third-order Birch-Murnaghan equation, yielding $V_0 = 435.49(3) \text{ \AA}^3$, $K_0 = 129(1) \text{ GPa}$, $K' = 2.7(3)$. The equation of state obtained by fixing $K' \equiv 4$ is similar, yielding $V_0 = 435.52(3) \text{ \AA}^3$, $K_0 = 123.7(3) \text{ GPa}$. The data were fitted using the Levenberg-Marquardt algorithm (Press et al. 1992). A statistical analysis of the fitted data provides an estimate of 0.05 GPa as the error in pressure. The data and the fitted curve are presented in Figure 2.

Axial compressibility

Unit-cell parameters decrease gradually with increasing pressure. No discontinuity was detected within the experimental

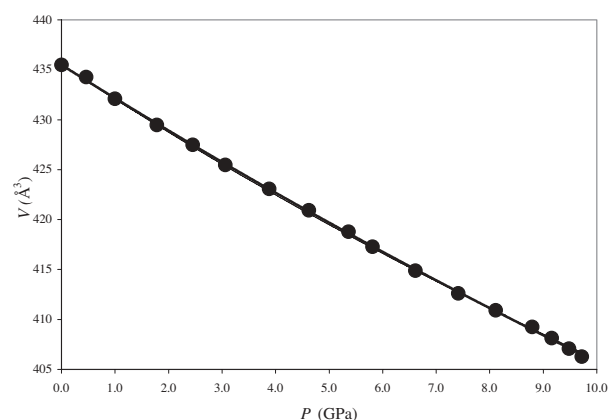


FIGURE 2. Variation of unit-cell volume of KCpx crystal with pressure. Fitted curve is a third order Birch-Murnaghan equation, with $V_0 = 435.49(3) \text{ \AA}^3$, $K_0 = 129(1) \text{ GPa}$, $K' = 2.7(3)$.

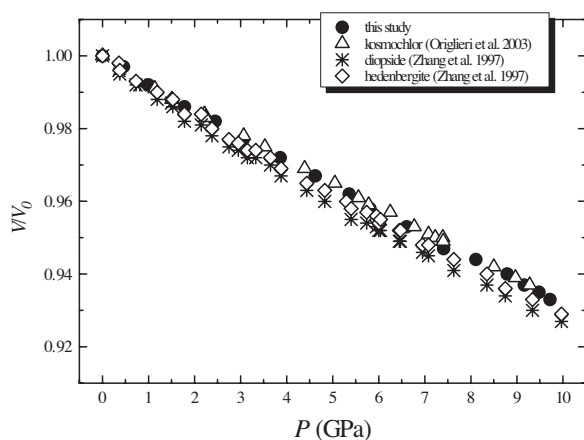


FIGURE 3. Pressure dependence of the unit-cell volumes for selected C2/c clinopyroxenes. For details see the legend.

uncertainty. As it is evident from Figure 3, the high-pressure unit-cell parameters of KCpx match those found for kosmochlor (Origlieri et al. 2003), but are stiffer than those observed for synthetic diopside and hedenbergite (Zhang et al. 1997). The axial compressibilities, β_a , β_b , and β_c , of the KCpx are $2.23(5)$, $2.76(4)$, and $2.25(4) \times 10^{-3} \text{ GPa}^{-1}$. These values are intermediate between those observed for kosmochlor and those for the diopside-hedenbergite join. In particular, the KCpx exhibits a compression of the **b**-axis about 15% greater than that of kosmochlor (Origlieri et al. 2003) and about 20% lower than that of hedenbergite (Zhang et al. 1997).

Unit strain ellipsoids

When dealing with monoclinic symmetry, unit strain analysis provides a clearer picture of the compression of the cell volume because the axes of the strain ellipsoid are not constrained to coincide with the **a** or **c** cell axes. Unit-strain ellipsoids were computed with the cell-parameter data between room and pressure conditions using Ohashi's STRAIN software (Hazen and Finger 1982), and are reported in Table 6. There is significant anisotropy of the unit strain ellipsoid, as demonstrated by the axial ratios of 1:1.94:1.90 computed in the range 0–9.72 GPa. As a function of pressure, there is a small change in the magnitude of the unit strain parallel to the stiffest direction, ϵ_1 , and very little change in its orientation, which approximately bisects the **a**- and **c**-axes. The other two ellipsoid axes are roughly equal in length and stiffen considerably with increasing pressure. The anisotropy of the unit-cell compression has been discussed by Zhang et al. (1997) and Tribaudino et al. (2000). Origlieri et al. (2003) demonstrated that the orientations of the ellipsoidal axes are related to directions of closest packing in pyroxenes. The strain ellipsoid for KCpx between 9.72 GPa and room conditions is illustrated in Figure 4, superimposed on a cartoon of the crystal structure oriented down **a*** with the **b**-axis horizontal.

Polyhedral compressibility

Compressibilities of the bond distances within the M2, M1, and T polyhedra show significant anisotropy. The compression most relevant to this study involves the M2-polyhedron. As usual for the high-pressure behavior of clinopyroxenes (Zhang et al.

TABLE 5. Electron microprobe analyses for KCpx (mean and ranges in wt% of oxides)

	939-1	Range
SiO ₂	54.85	53.98–55.12
Al ₂ O ₃	4.46	3.85–4.68
MgO	15.42	15.25–15.99
CaO	22.75	21.98–23.02
K ₂ O	2.60	2.45–2.81
Total	100.08	
T site		
Si	1.98	
Al	0.02	
M1 site		
Mg	0.83	
Al	0.17	
M2 site		
Ca	0.88	
K	0.12	
Charge	12.03	

Note: *n* is the number of analyses on different spots; *n* = 10.

1997; Arlt and Angel 2000; Origlieri et al. 2003), the longest bond lengths, M2O3(c,d), show a marked shortening in the range of pressure investigated. The longest bond pair, M2O3d, undergoes a compression of 5.8(4)% whereas the compression of M2O3c is only 2.0(4)%. Because of the higher compression of M2O3d, this distance approaches the value of M2O3c at higher pressure. This structural change is represented by the variation of the Δ parameter (Table 4), defined as $\Delta = [R(\text{M2O3d}) - R(\text{M2O3c})]$, in the range of pressure studied. Thompson and Downs (2004) show that the shortening of M2O3d is concomitant with the rotation of the SiO_4 tetrahedron. Harlow (1997) suggested that K-O bond lengths compress significantly with pressure and therefore at elevated pressures the K atom may be small enough to fit into the pyroxene structure with greater ease than at room pressures. Indeed, Hazen and Finger (1978), in their study of the compression of phlogopite, concluded that the K-O bond length was the most compressible of all oxide bond lengths. There are several recent studies of K-bearing phases at pressure from which one can estimate the compressibility of the K-O bond. These include phlogopite (Comodi et al. 2004), kalicinite (Kagi et al. 2003) and microcline (Allan and Angel 1997). The variations of the average M2-O bond length of KCpx over the pressure range of the experiment as well as the expected variation of the average K-O

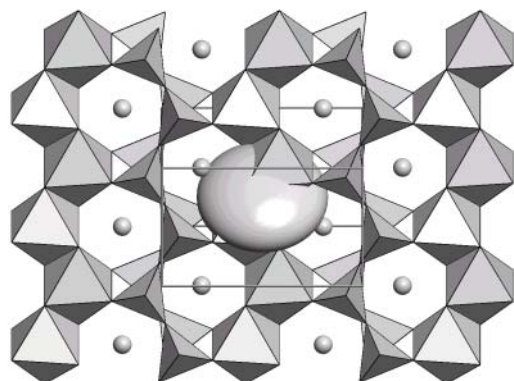


FIGURE 4. Oriented unit strain ellipsoid for KCpx overlaying a depiction of the KCpx structure viewed down a^* , with the b axis horizontal. M1O_6 and SiO_4 are rendered as polyhedra and M2 as a sphere.

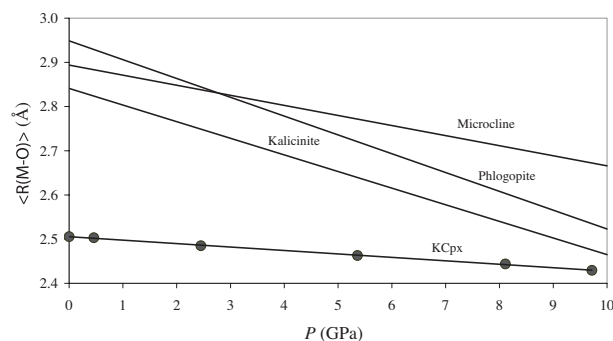


FIGURE 5. Variation of the average M2-O bond length over the pressure range of the experiment as well as the expected variation of the average K-O bond lengths, $\langle R(\text{K-O}) \rangle$, for kalicinite (Kagi et al. 2003), phlogopite (Comodi et al. 2004), and microcline (Allan and Angel 1997).

bond lengths, $\langle R(\text{K-O}) \rangle$, for phlogopite, kalicinite, and microcline are illustrated in Figure 5. The greatest change observed in these structures for K-O bond lengths is observed in phlogopite, displaying 7.2% compression, followed by kalicinite at 6% and microcline at 4%. It is evident that the K-O bond compresses more than the M2-O bond found in the KCpx studied here and supports the conjecture of Harlow (1997) that “the K atom is softer” than the bulk M2 polyhedron and thus shrinks enough at high pressure to fit into the pyroxene structure.

Although less pronounced, the variations in the M1 polyhedra are also meaningful. The three bond pairs display anisotropic compression, as well. The M1O_6 volume compression for KCpx (8.2%) is lower than diopside (9.4%, extrapolated; Levien and Prewitt 1981), but higher than observed for hedenbergite (6.6%; Zhang et al. 1997), spodumene (6.1%, extrapolated; Arlt and Angel 2000) or kosmochlor (5.0%; Origlieri et al. 2003) over a comparable pressure range. Thus, the M1 polyhedron of KCpx is more compressible than FeO_6 , AlO_6 , and CrO_6 octahedra, but less than MgO_6 .

Significant anisotropic compression is also found for the TO_4 tetrahedron. The longest Si-O3b bond length is not the most compressible (Zhang et al. 1997). The longest, Si-O3b, and second longest, Si-O3a distances compress by 0.7(4) and 0.8(4)%, respectively. The compressions of the shortest, Si-O2, and the second shortest, Si-O1, bonds are 0.2(5) and 0.9(5)%, respectively. Figure 6 shows the variation of the O3-O3-O3 angle as a function of pressure. The O3-O3-O3 angle defines the extension of the pyroxene silicate chain and can be determined by the angle between the basal edge of a tetrahedron and (100) (Thompson 1970; Cameron et al. 1973). Our data show a linear trend ($R^2 = 0.993$) and can be approximated by an equation $\text{O3-O3-O3} = 167.23(8) - 0.36(1)P$ (GPa). The decrease in the kinking angle indicates that the silicate chains become less extended with pressure (Origlieri et al. 2003). The value of O3-O3-O3, 167.17(8) in KCpx at room conditions, is intermediate between those observed in kosmochlor, 172.8(2) (Origlieri et al. 2003) and hedenbergite, 164.4(2) (Zhang et al. 1997), whereas it is close to the value found in diopside, 166.37(6) (Levien and Prewitt 1981).

Figure 7 shows the variation of the Si-O3-Si angle with pressure. A linear trend is observed ($R = 0.991$) as well. It can be approximated by an equation: $\text{Si-O3-Si} = 136.5(1) - 0.30(2)P$ (GPa). We observed a continuous variation of this angle by 3.0° [2.1(3)%]. Hence, the rotation of the SiO_4 tetrahedron around the normal to the tetrahedral basal plane accompanies the continuous kinking.

Influence of potassium incorporation on elasticity and structural compression

Thompson et al. (2005) show that the volume compressibility of $C2/c$ pyroxenes can be described as a function of two factors: the compressibility of the M1 site and the value of the O3-O3-O3 angle at ambient conditions. The compressibility of the M1 site is related to the size of the M1 cation; the smaller the cation radius, the smaller the volume of the unit cell and the larger the bulk modulus. As the O3-O3-O3 angle decreases, the cell volume and compressibility decrease. Since CrO_6 and AlO_6 octahedra are less compressible than FeO_6 and MgO_6 octahedra, the bulk modulus

TABLE 6. Unit strain ellipsoids as a function of pressure computed with Ohashi's STRAIN software

P (GPa)	1.78	2.45	3.06	3.86	4.62	5.36	5.81	6.61	8.11	8.79	9.16	9.48	9.72
$-\varepsilon_1$	0.136(4)	0.136(3)	0.137(2)	0.138(2)	0.137(1)	0.138(1)	0.140(1)	0.143(1)	0.143(1)	0.142(1)	0.142(1)	0.1434(9)	0.1456(7)
$-\varepsilon_2 // \mathbf{b}$	0.315(3)	0.302(2)	0.306(1)	0.298(1)	0.294(1)	0.291(1)	0.296(1)	0.292(2)	0.289(4)	0.280(2)	0.2770(9)	0.2827(9)	0.2827(6)
$-\varepsilon_3$	0.327(3)	0.315(2)	0.315(2)	0.307(1)	0.300(1)	0.295(1)	0.293(2)	0.293(1)	0.289(4)	0.278(2)	0.282(1)	0.278(1)	0.2773(7)
$\angle \varepsilon_1 \wedge \mathbf{a}$ ($^\circ$)	54.5(8)	53.8(7)	53.7(5)	53.1(4)	53.5(4)	53.3(3)	53.1(3)	53.2(2)	53.1(2)	52.9(2)	52.3(3)	52.7(2)	52.8(2)
$\angle \varepsilon_1 \wedge \mathbf{c}$ ($^\circ$)	51.5(8)	52.2(7)	52.3(5)	51.9(4)	52.5(3)	52.7(3)	52.9(3)	52.8(2)	52.8(2)	53.1(2)	53.7(3)	53.3(2)	53.2(2)
$\angle \varepsilon_2 \wedge \mathbf{a}$ ($^\circ$)	144.5(8)	143.8(7)	143.7(5)	144.0(4)	143.5(4)	143.3(4)	143.1(3)	143.2(4)	143(1)	142.9(7)	142.3(4)	142.7(3)	142.8(2)
$\angle \varepsilon_2 \wedge \mathbf{c}$ ($^\circ$)	38.5(8)	37.8(7)	37.7(5)	38.1(4)	37.5(4)	37.3(4)	37.1(3)	37.2(4)	37(1)	36.9(6)	36.4(4)	36.7(3)	36.8(2)

Notes: The strain was computed between room conditions and P . The axis labeled ε_2 is parallel to the \mathbf{b} axis. The magnitudes of ε have been multiplied by 100.

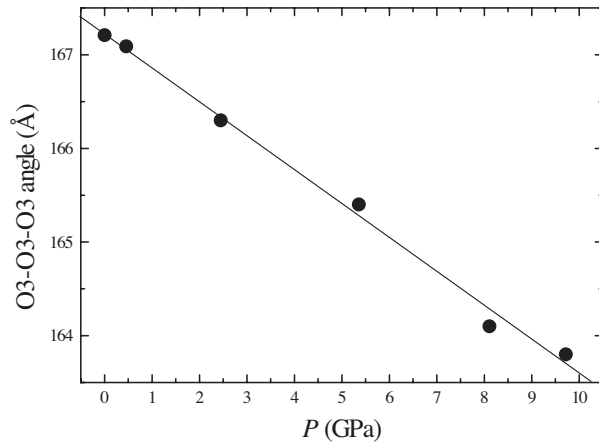


FIGURE 6. Variation of the O3-O3-O3 angle in KCpx as a function of pressure at 298 K.

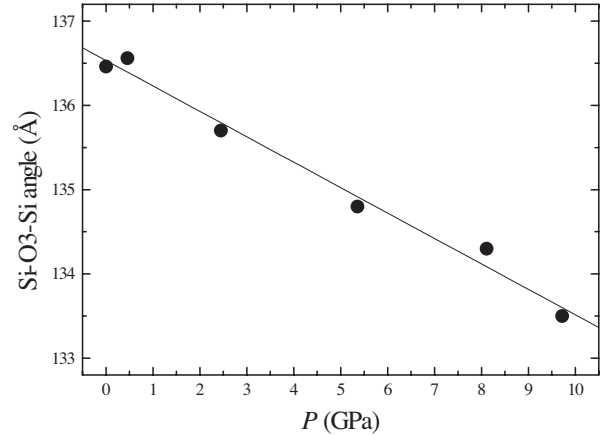


FIGURE 7. Variation of the Si-O3-Si angle in KCpx as a function of pressure at 298 K.

of KCpx should be intermediate between the bulk moduli of the structures with M^{2+} cations in the M1 site vs. those with M^{3+} cations. Examining the relationship between unit-cell volume at ambient condition and polyhedral cation radius for 22 $C2/c$ end-member silicate pyroxene crystal structures, Thompson et al. (2005) show that the M1 cation radii display a linear correlation with unit-cell volume whereas the effect of the M2 radius (from 0.60 to 1.12 Å) is not clear. Indeed, the unit-cell volume varies only by 3% as a function of the M2 radius.

Model unit-cell volumes for KCpx at different pressures were calculated using the formula proposed by Thompson and Downs (2004),

$$V = [32\sqrt{2}(1 - \cos\theta) + 64(1 - \cos\theta)^{3/2}/\sqrt{3}]r^3 \quad (1)$$

by combining the simple modeling of θ and r as quadratic in P , where θ is the O3-O3-O3 angle and r is an estimate of the radius of the O atom. Following Thompson et al. (2005), the volume-pressure relationships were derived from a simple set of equations: $r = m_1P^2 + m_2P + r_0$, and $\theta = m_1P^2 + m_2P + \theta_0$, where P is the pressure in GPa and the coefficients are given in Table 5 of Thompson et al. (2005) for $C2/c$ pyroxenes with Mg and Al in the M1 sites. The value for r_0 is obtained by solving Equation 1 using the observed value of θ and the observed unit-cell volume at room pressure. Two sets of volumes are computed, V_{diopside} and V_{jadeite} , representing the Mg and Al containing clinopyroxenes, and the unit-cell volume for the KCpx of the present study is then $V_{\text{KCpx}} = 0.83V_{\text{diopside}} + 0.17V_{\text{jadeite}}$. Thompson et al. (2005) showed that the excess of volume of mixing is negligibly small

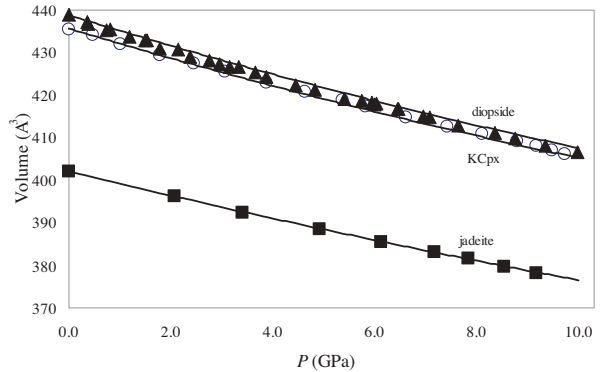


FIGURE 8. Variation of the observed (open circles = KCpx; filled symbols = jadeite and diopside) and modeled unit-cell volumes (lines). Upward triangles and squares refer to model volumes calculated with coefficient sets for $C2/c$ pyroxenes with Mg and Al in the M1 sites, respectively (Thompson et al. 2005).

in clinopyroxenes, and so the two volumes can simply be added together with weights equal to their chemical molar fractions. The results are summarized in Figure 8, where the model volumes are rendered with lines and the observed cell volumes are plotted for KCpx, jadeite, and diopside. It is evident that the observed volumes for KCpx are very close to those calculated with the coefficient sets for Mg-containing diopside. As can be seen from this plot, the coupled substitution of KAl for CaMg results in an increase of the bulk modulus over the diopside value. This is consistent with the modeling of Thompson and Downs (2004)

and Thompson et al. (2005) who conclude that it is the compressibility of the $M1O_6$ group that controls compressibility in the pyroxenes and not the chemistry of the $M2$ polyhedron. Thus, we conclude that the incorporation of K into the clinopyroxene structure has little effect on its compressibility, although the concomitant Al in $M1$ from the K-Jd component does reduce its compressibility. Potassium dilates the $M2$ polyhedron and V_0 at ambient conditions, as shown by Bindi et al. (2002) and Harlow (1996), but other than this effect does not play a noticeable role in the compressibility.

ACKNOWLEDGMENTS

Authors thank Filippo Olmi (CNR-Istituto di Geoscienze e Georisorse sez. di Firenze) for his help in the microprobe analyses. The study is supported by M.I.U.R., P.R.I.N. 2003, project "Structural complexity in minerals: modularity and modulations," the Italian CNR-Istituto di Geoscienze e Georisorse sez. di Firenze, the Russian Foundation for Basic Research (projects 04-05-64896 to OGS, 02-05-64684 to Y.A.L., and 02-05-64025 to L.L.P.), the RF President's Leading Scientific Schools Program (project no. 1645.2003.5 to L.L.P.), the RAS project no. 7 for High-Pressure Research (to Y.A.L.), and the Europea Academia (to O.G.S.). Funding from the National Science Foundation for the Study of Compression Mechanisms of Upper Mantle Minerals, EAR-9903104, to Downs and Uchida is gratefully acknowledged.

REFERENCES CITED

- Albee, A.L. and Ray, L. (1970) Correction factors for electron probe analysis of silicate, oxides, carbonates, phosphates, and sulphates. *Analytical Chemistry*, 48, 1408–1414.
- Allan, D.R. and Angel, R.J. (1997) A high-pressure structural study of microcline ($KAlSi_3O_8$) to 7 GPa. *European Journal of Mineralogy*, 9, 263–275.
- Angel, R.J., Downs, R.T., and Finger, L.W. (2000) High-temperature high-pressure diffraction. In R.M. Hazen and R.T. Downs, Eds., *High-Temperature and High-Pressure Crystal Chemistry*, 41, p. 559–596. Reviews in Mineralogy and Geochemistry, Mineralogical Society of America, Chantilly, Virginia.
- Arlt, T. and Angel, R.J. (2000) Displacive phase transitions in C-centred clinopyroxenes: spodumene, $LiScSi_2O_6$ and $ZnSiO_3$. *Physics and Chemistry of Minerals*, 27, 719–731.
- Bence, A.E. and Albee, A.L. (1968) Empirical correction factors for the electron microanalysis of silicate and oxides. *Journal of Geology*, 76, 382–403.
- Bindi, L., Safonov, O.G., Litvin, Y.A., Perchuk, L.L., and Menchetti, S. (2002) Ultrahigh potassium content in the clinopyroxene structure: an X-ray single-crystal study. *European Journal of Mineralogy*, 14, 929–934.
- Bindi, L., Safonov, O.G., Yapaskurt, V., Perchuk, L.L., and Menchetti, S. (2003) Ultrapotassic clinopyroxene from the Kumdy-Kol microdiamond min, Kokchetav Complex, Northern Kazakhstan: occurrence, composition and crystal-chemical characterization. *American Mineralogist*, 88, 464–468.
- Bishop, F.C., Smith, J.V., and Dawson, J.B. (1978) Na, K, P and Ti in garnet, pyroxene and olivine from peridotite and eclogite xenoliths from African kimberlites. *Lithos*, 11, 155–173.
- Cameron, M., Sueno, S., Prewitt, C.T., and Papike, J.J. (1973) High-Temperature crystal chemistry of amcrite, diopside, hedenbergite, jadeite, spodumene, and ureyite. *American Mineralogist*, 58, 594–618.
- Chudinovskikh, L.T., Zharikov, V.A., Ishbulatov, R.A., and Matveev, Yu.A. (2001) On the mechanism of incorporation of ultra-high amounts of potassium into clinopyroxene at high pressure. *Doklady Rossiiskoi Akademii Nauk, Earth Sciences*, 380, 1–4.
- Comodi, P., Fumagalli, P., Montagnoli, M., and Zanazzi, P.F. (2004) A single-crystal study on the pressure behavior of phlogopite and petrological implications. *American Mineralogist*, 89, 647–653.
- Downs, R.T. and Hall-Wallace, M. (2003) The American Mineralogist crystal structure database. *American Mineralogist*, 88, 247–250.
- Edgar, A.D. and Vukadinovic, D. (1993) Potassium-rich clinopyroxene in the mantle: an experimental investigation of K-rich lamproite up to 60 kbar. *Geochimica et Cosmochimica Acta*, 57, 5063–5072.
- Finger, L.W. and Prince, E. (1975) A system of Fortran IV computer programs for crystal structure computations. U.S. Bureau of National Standards Technical Note 854, 128 p.
- Ghorbani, M.R. and Middlemost, E.A.K. (2000) Geochemistry of pyroxene inclusions from the Warrumbungle Volcano, New South Wales, Australia. *American Mineralogist*, 85, 1349–1367.
- Hamilton, D.L. and Henderson, C.M.B. (1968) The preparation of silicate compositions by a gelling method. *Mineralogical Magazine*, 36, 832–838.
- Harlow, G.E. (1996) Structure refinement of a natural K-rich diopside: the effect of K on the average structure. *American Mineralogist*, 81, 632–638.
- — — (1997) K in clinopyroxene at high pressure and temperature: an experimental study. *American Mineralogist*, 82, 259–269.
- Harlow, G.E. and Veblen, D.R. (1991) Potassium in clinopyroxene inclusions from diamonds. *Science*, 251, 652–655.
- Hazen, R.M. and Finger, L.W. (1978) The crystal structures and compressibilities of layer minerals at high pressure. II. Phlogopite and chlorite. *American Mineralogist*, 63, 293–296.
- — — (1982) *Comparative crystal chemistry*, 231 p. John Wiley and Sons, New York.
- Ibers, J.A. and Hamilton, W.C., Eds. (1974) *International Tables for X-ray Crystallography*, vol. IV, 366 p. Kynock, Dordrecht.
- Jaques, A.L., O'Neill, H.St.C., Smith, C.B., Moon, J., and Chappell, B.W. (1990) Diamondiferous peridotite xenoliths from the Argyle (AK1) lamproite pipe, Western Australia. *Contributions to Mineralogy and Petrology*, 104, 255–276.
- Kagi, H., Nagai, T., Loveday, J.S., Wada, C., Parise, J.B. (2003) Pressure-induced phase transformation of kalicinite ($KHCO_3$) at 2.8 GPa and local structural changes around hydrogen atoms. *American Mineralogist*, 88, 1446–1451.
- King, H.E. and Finger, L.W. (1979) Diffracted beam crystal centering and its application to high-pressure crystallography. *Journal of Applied Crystallography*, 12, 374–378.
- Levien, L. and Prewitt, C.T. (1981) High pressure structural study of diopside. *American Mineralogist*, 66, 315–323.
- Litvin, Y.A. (1990) Physical and chemical studies of melting of materials from the Deep Earth, 312 p. Nauka, Moscow (in Russian).
- Mao, H.K., Bell, P.M., Shaner, J.W., and Steinberg, D.J. (1978) Specific volume measurements of Cu, Mo, Pd, and Ag and calibration of the ruby R₁ fluorescence pressure gauge from 0.06 to 1 Mbar. *Journal of Applied Physics*, 49, 3276–3283.
- Origlieri, M.J., Downs, R.T., Thompson, R.M., Pommier, C.J.S., Denton, M.B., and Harlow, G.E. (2003) High-pressure crystal structure of kosmochlor, $NaCrSi_2O_6$, and systematics of anisotropic compression in pyroxenes. *American Mineralogist*, 88, 1025–1032.
- Perchuk, L.L., Sobolev, N.V., Yapaskurt, V.O., and Shatsky, V.S. (1996) Relics of potassium-bearing pyroxenes from diamond-free pyroxene-garnet rocks of the Kokchetav massif, northern Kazakhstan. *Doklady Rossiiskoi Akademii Nauk*, 348, 790–795.
- Perchuk, L.L., Safonov, O.G., Yapaskurt, V.O., and Barton, J.M., Jr. (2002) Crystal-melt equilibria involving potassium-bearing clinopyroxene as indicators of mantle-derived ultrahigh-potassic liquids: an analytical review. *Lithos*, 60(3–4), 89–111.
- Press, W.H., Teukolsky, S.A., Vetterling, W.T., and Flannery, B.P. (1992) *Numerical Recipes in Fortran*, 963 p. Cambridge University Press.
- Reid, A.M., Brown, R.W., Dawson, J.B., Whitfield, G.G., and Siebert, J.C. (1976) Garnet and pyroxene compositions in some diamondiferous eclogites. *Contributions to Mineralogy and Petrology*, 58, 203–220.
- Safonov, O.G., Matveev, Y.A., Litvin, Yu.A., and Perchuk, L.L. (2002) Experimental study of some joins of the system $CaMgSi_2O_6$ -(Ca,Mg)₃Al₂Si₂O₁₂-KAlSi₃O₈-K₂(Ca,Mg)(CO₃)₂ at 5–7 GPa in relation to the genesis of garnet-clinopyroxene-carbonate rocks of the Kokchetav Complex (Northern Kazakhstan). *Petrology*, 10, 519–539.
- Safonov, O.G., Litvin, Yu.A., Perchuk, L.L., Bindi, L., and Menchetti, S. (2003) Phase relations of potassium-bearing clinopyroxene in the system $CaMgSi_2O_6$ -KAlSi₃O₈ at 7 GPa. *Contribution to Mineralogy and Petrology*, 146, 120–133.
- Safonov, O.G., Perchuk, L.L., Litvin, Yu.A., and Bindi, L. (2005) Phase relations in the $CaMgSi_2O_6$ -KAlSi₃O₈ join at 6 and 3.5 GPa as a model for formation of some potassium-bearing deep-seated mineral assemblages. *Contributions to Mineralogy and Petrology*, 149, 316–337.
- Sobolev, N.V. and Shatsky, V.S. (1990) Diamond inclusions in garnets from metamorphic rocks: a new environment for diamond formation. *Nature*, 343, 742–746.
- Thompson, J.B., Jr. (1970) Geometrical possibilities for amphibole structures: model biopyriboles. *American Mineralogist*, 55, 292–293.
- Thompson, R.M. and Downs, R.T. (2004) Model pyroxenes II: Structural variation as a function of tetrahedral rotation. *American Mineralogist*, 89, 614–628.
- Thompson, R.M., Downs, R.T., and Redhammer, G.J. (2005) Model pyroxenes III: Volume of C2/c pyroxenes at mantle P, T, and x. *American Mineralogist*, 90, 1840–1851.
- Tribaudino, M., Prencipe, M., Bruno, M., and Levy, D. (2000) High-pressure behaviour of Ca-rich C2/c clinopyroxenes along the join diopside-enstatite ($CaMgSi_2O_6$ -Mg₂Si₂O₆). *Physics and Chemistry of Minerals*, 27, 656–664.
- Zhang, L., Ahsbahs, H., Hafner, S.S., and Kutoglu, A. (1997) Single-crystal compression and crystal structure of clinopyroxene up to 10 GPa. *American Mineralogist*, 82, 245–258.

MANUSCRIPT RECEIVED JULY 7, 2005

MANUSCRIPT ACCEPTED DECEMBER 25, 2005

MANUSCRIPT HANDLED BY KEVIN ROSSO